Location of the Hole and Acid Proton in Neutral Nonprotonated and Protonated Mixed (Phthalocyaninato)(porphyrinato) Yttrium Double-Decker Complexes: Density Functional Theory Calculations

Yuexing Zhang, Xue Cai, Ping Yao, Hui Xu, Yongzhong Bian, and Jianzhuang Jiang*[a]

Abstract: The location of the hole and acid proton in neutral nonprotonated and protonated mixed (phthalocyaninato)(porphyrinato) yttrium double-decker complexes, respectively, is studied on the basis of density functional theory (DFT) calculations on the molecular structures, molecular orbitals, atomic charges, and electronic absorption and infrared spectra of the neutral, reduced, and two possible protonated species of a mixed (phthalocyaninato)-(porphyrinato) yttrium compound: [(Pc)Y(Por)], [(Pc)Y(Por)]$^-$, [(HPc)Y-(Por)], and [(Pc)Y(HPor)], respectively. When the neutral [(Pc)Y(Por)] is reduced to [(Pc)Y(Por)]$^-$, the calculated results on the molecular structure, atomic charge, and electronic absorption and infrared spectra show that the added electron has more influence on the Pc ring than on its Por counterpart, suggesting that the location of the hole is on the Pc ring in neutral [(Pc)Y-(Por)]. Nevertheless, comparison of the calculation results on the structure, orbital composition, charge distribution, and electronic absorption and infrared spectra between [(HPc)Y(Por)] and [(Pc)Y(HPor)] leads to the conclusion that the acid proton in the protonated mixed (phthalocyaninato)(porphyrinato) yttrium compound should be localized on the Por ring rather than the Pc ring, despite the localization of the hole on the Pc ring in [(Pc)Y(Por)]. This result is in line with the trend revealed by comparative studies of the X-ray single-crystal molecular structures between [M^{III}{Pc(α-OC$_5$H$_{11}$)$_4$}-(TClPP)] and [M^{III}H{Pc(α-OC$_5$H$_{11}$)$_4$}-(TClPP)] (H$_2$TClPP = 5,10,15,20-tetrakis(4-chlorophenyl)porphyrin; M = Sm, Eu). The present work not only represents the first systemic DFT study on the structures and properties of mixed (phthalocyaninato)(porphyrinato) yttrium double-decker complexes, but more importantly sheds further light on the nature of protonated bis(tetrapyrrole) rare-earth complexes.

Keywords: density functional calculations · phthalocyanines · porphyrinoids · yttrium

Introduction

Porphyrins (Por) and phthalocyanines (Pc), as the most common and important tetrapyrrole derivatives, have been at the focus of multidisciplinary interest for more than a century.[1–4] Both series of macrocycles can form complexes with almost all the metals in the periodic table. It is known that rare earths, actinides, and some early transition metals and main-group metal elements can form sandwich-type complexes with these ligands in the form of double- and triple-decker complexes.[5] These sandwich-type tetrapyrrole metal complexes, in particular bis- and tris(tetrapyrrole) rare-earth complexes, have been emerging as an important class of functional materials in the fields of molecular electronics, molecular information storage, nonlinear optics, and organic field-effect transistors, due to their intriguing and unique electronic and optical properties.[1,5a–c,6]

Due to the fact that all the rare-earth elements (except for cerium) usually take the tervalent oxidation state, and both phthalocyanine and porphyrin need two electrons to form 18-electron π systems in the dianion form, neutral bis-(tetrapyrrole) rare-earth double-decker complexes, including [M^{III}(Pc)$_2$], [M^{III}(Por)$_2$], and [(Pc)M^{III}(Por)], with a hole in one of the two tetrapyrrole rings are easily transformed into the form of [(P)M(P′)]$^-$ or [(P)M(HP′)] (P = or ≠ P′ = tetrapyrrole) on the basis of reduction.[5h,7] As a result, much effort has been spent to try to determine the location of the hole and acid proton in corresponding bis(tetrapyrrole) rare-earth(III) double-decker complexes, due to the important role of the hole and/or proton in materials science.[5h,7]

[a] Y. Zhang, X. Cai, P. Yao, H. Xu, Dr. Y. Bian, Prof. J. Jiang
Key Lab for Colloid and Interface Chemistry of Education Ministry
Department of Chemistry, Shandong University
Jinan 250100 (P. R. China)
Fax: (+86)531-8856-5211
E-mail: jzjiang@sdu.edu.cn

Supporting information for this article is available on the WWW under http://www.chemeurj.org/ or from the author.

The X-ray diffraction technique did not give any effective information about the location of either the hole or the acid proton in such compounds. However, vibrational spectroscopy, in particular the IR technique, has been proved to be reliable in determining the location of the hole.[5a–c,7i] On the vibrational timescale the hole has been revealed to delocalize over both the rings in the double-deckers consisting of two tetrapyrrole ligands with similar electrochemical characteristics, such as homoleptic [M(Pc)$_2$],[8] [M{Pc(C$_7$H$_{15}$)$_8$}$_2$],[9] [M{Pc(OC$_n$H$_{2n+1}$)$_8$}$_2$] ($n=5$, 8),[9c,10] [M{Pc(α-OC$_5$H$_{11}$)$_4$}$_2$],[5g] [M(oep)$_2$] (H$_2$oep = 2,3,7,8,12,13,17,18-octaethylporphin),[11] and mixed ring [M(Nc)(oep)] (Nc = 2,3-naphthalocyaninate).[5e] It is worth noting that in the mixed ring bis(tetrapyrrole) rare-earth double-decker compounds, the hole is usually located on the tetrapyrrole with a HOMO energy significantly lower than the other one. For example, the hole was verified to reside on the Pc ring in [M(Pc)(TClPP)] (H$_2$TClPP = 5,10,15,20-tetrakis(4-chlorophenyl)porphyrin) according to the IR spectroscopic result.[7i] However, the location of acid proton in protonated bis(tetrapyrrole) rare-earth complexes, in particular the mixed (phthalocyaninato)(porphyrinato) rare-earth compounds, has not yet been determined thus far by experimental techniques.[5h]

In the present paper, density functional theory (DFT) calculations at the B3LYP[12] level with the LANL2DZ basis set[13] on the structures, molecular orbitals, atomic charges, electronic absorption spectra, and infrared spectra of neutral non-protonated, [(Pc)Y(Por)], and reduced, [(Pc)Y(Por)]$^-$, forms of the mixed (phthalocyaninato)(porphyrinato) yttrium double-decker complex have been carried out. To determine the location of the acid proton atom in the protonated mixed (phthalocyaninato)(porphyrinato) yttrium complex, similar calculations on the two possible protonated species [(HPc)Y(Por)] and [(Pc)Y(HPor)] were also carried out. Comparison of the calculated results between [(Pc)Y(Por)] and [(Pc)Y(Por)]$^-$ and between [(HPc)Y(Por)] and [(Pc)Y(HPor)], in particular with the help of experimental findings, leads to the conclusion that the hole presides on the Pc ring in neutral [(Pc)Y(Por)] and the acid proton is located on the Por ligand in protonated [(Pc)Y(HPor)]. To the best of our knowledge, this represents the first effort toward understanding the structure and properties of mixed (phthalocyaninato)(porphyrinato) rare-earth double-decker complexes on the basis of DFT calculations.

Results and Discussion

Molecular structures: Figure 1 shows the optimized structures of [(Pc)Y(Por)] together with the position of the acid proton in [(HPc)Y(Por)] and [(Pc)Y(HPor)]. The energy-minimized structures for both [(Pc)Y(Por)] and [(Pc)Y(Por)]$^-$ optimized at the B3LYP/LANL2DZ level are of C_{4v} symmetry. In [(Pc)Y(Por)] and [(Pc)Y(Por)]$^-$, the yttrium atom is sandwiched between two distorted tetrapyrrole (Pc and Por) rings with a twist angle of 45° (note that the twist angle is defined as the rotation angle of one macrocycle
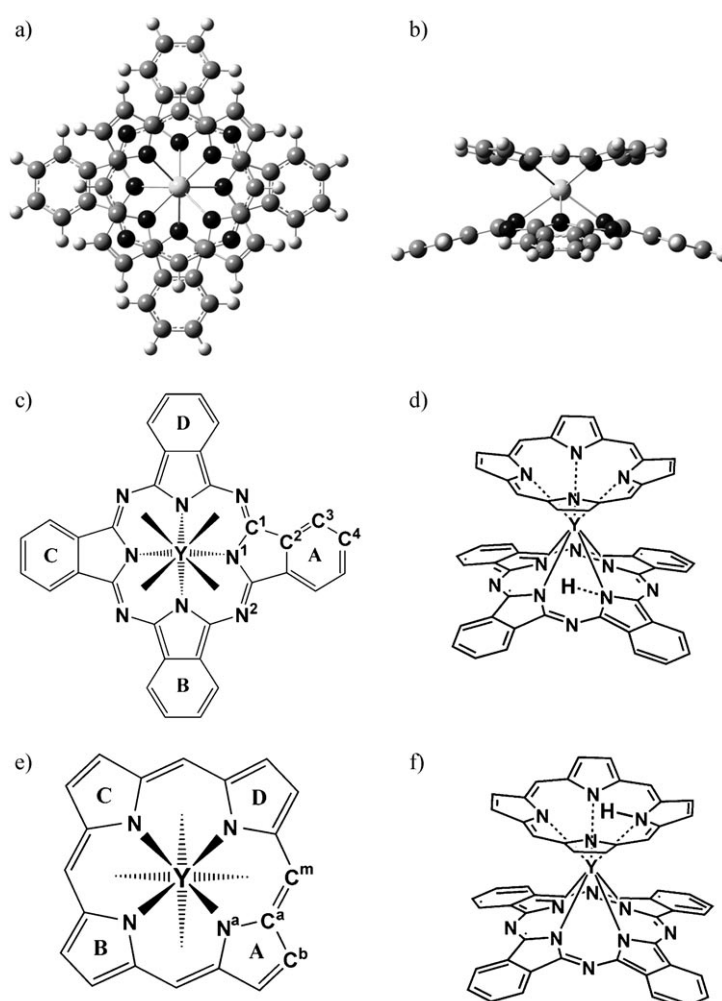

Figure 1. Optimized structures (a, b) and atomic labeling (c, e) of [(Pc)Y-(Por)], and the position of the acid proton in [(HPc)Y(Por)] (d) and [(Pc)Y(HPor)] (f).

away from the eclipsed conformation of the two macrocycles). As a consequence, both neutral [(Pc)Y(Por)] and reduced [(Pc)Y(Por)]$^-$ adopt a square antiprismatic coordination structure around the yttrium metal center formed by four isoindole nitrogen atoms (N$^{1A–D}$) of the Pc ring and four pyrrole nitrogen atoms (N$^{aA–D}$) of the Por ring. In contrast, in the energy-minimized structures of the two possible protonated forms of the double-decker complex, [(HPc)Y-(Por)] and [(Pc)Y(HPor)], the relatively higher C_{4v} symmetry disappears due to the significant deviation of the isoindole nitrogen atom N^{1A} from the mean plane formed by the four isoindole nitrogen atoms (N$^{1A–D}$) in the Pc ring and the pyrrole nitrogen atom N^{aA} from the mean plane formed by the four pyrrole nitrogen atoms (N$^{aA–D}$) in the Por ring. Calculation results indicate that the energy-minimized structures of both [(HPc)Y(Por)] and [(Pc)Y(HPor)] take an approximate C_s symmetry. It is worth noting that the absence of an imaginary vibration predicted in the following frequency calculations of the infrared vibrational spectra con-

firms that the energy-minimized structures for all the four forms of yttrium double-decker compounds are true energy minima. In addition, it is also worth pointing out that the efficiency of the B3LYP method and LANL2DZ basis set in calculating bis(tetrapyrrole) rare-earth systems has been proved by the previous study on the bis(phthalocyaninato) yttrium compound.[8d]

As tabulated in Table S1 (Supporting Information), introducing one electron to the semi-occupied HOMO of the neutral species [(Pc)Y(Por)], and thus reducing it to a closed-shell system [(Pc)Y(Por)]$^-$, induces many changes in the structure of the double-decker molecule according to the calculated results. Along with the reduction of [(Pc)Y(Por)] to [(Pc)Y(Por)]$^-$, the distance between the N$^{1A–D}$ and N$^{aA–D}$ planes increases from 2.727 to 2.772 Å, indicating the relatively weaker interring π–π interaction in [(Pc)Y(Por)]$^-$ compared to [(Pc)Y(Por)]. However, in line with both the experimental findings and calculated results on bis(phthalocyaninato) yttrium complexes [Y(Pc)$_2$] and [Y(Pc)$_2$]$^-$,[8d] reduction of [(Pc)Y(Por)] to [(Pc)Y(Por)]$^-$ leads to very small structural changes in either bond lengths or bond angles for both the Pc and Por rings on the basis of the calculation results (Table S1, Supporting Information). As a consequence, the relatively larger increase in the distance between the two neighboring isoindole nitrogen atoms N^{1A}···N^{1B} in the Pc ring compared to N^{aA}···N^{aB} in the Por ring along with the reduction, 0.01 Å versus 0.004 Å, therefore suggests that the electron added into the semi-occupied HOMO of [(Pc)Y-(Por)] exerts more influence on the Pc ring than on the Por ring in terms of the molecular structure change. This in turn suggests that the hole localizes on the Pc ring instead of the Por ring in the neutral nonprotonated mixed (phthalocyaninato)(porphyrinato) yttrium double-decker complex.

To determine the location of the acid proton in the protonated mixed (phthalocyaninato)(porphyrinato) yttrium complex, the structures of two possible protonated species, namely [(HPc)Y(Por)] and [(Pc)Y(HPor)], were also calculated. The results show that in comparison with the introduction of one electron into the semi-occupied HOMO of [(Pc)Y(Por)], incorporating one hydrogen atom {actually one electron into the semi-occupied HOMO of [(Pc)Y(Por)] and one proton to either the Pc or Por ring} induces more significant changes in the molecular structure of both the tetrapyrrole rings in the double-decker molecule. In the case that the acid proton is attached onto the Pc ring and connected with one of the four isoindole nitrogen atoms (N^{1A}) the N$^{1A–D}$ plane formed by the four isoindole nitrogen atoms in [(HPc)Y(Por)] distorts with a N^{1A}-N^{1B}-N^{1D}-N^{1C} dihedral angel of 175°, while the N$^{aA–D}$ plane formed by the four pyrrole nitrogen atoms in the Por ring remains coplanar. Due to the repulsion between the acid proton and yttrium, the distance from yttrium to the mean N$^{1A–D}$ plane, which is defined as the average distance from yttrium to the N^{1ABD} and N^{1BDC} planes, in [(HPc)Y(Por)] increases by 0.299 Å relative to that in [(Pc)Y(Por)], whereas the distance from yttrium to the N$^{aA–D}$ plane decreases by 0.146 Å. Similarly, incorporating the proton in the Por ring leads to the deviation of

the N$^{aA–D}$ plane in the Por ring from coplanar to a N^{aA}-N^{aB}-N^{aD}-N^{aC} dihedral angel of 176° in [(Pc)Y(HPor)], while the N$^{1A–D}$ plane in the Pc ring remains coplanar. Repulsion between the proton and yttrium in [(Pc)Y(HPor)] leads to a increase of 0.327 Å in the distance from yttrium to the mean N$^{aA–D}$ plane and a small decrease of 0.189 Å in the distance from yttrium to the N$^{1A–D}$ plane in [(Pc)Y(HPor)] relative to the distances in [(Pc)Y(Por)]. According to these calculation results, changes in the molecular structure of mixed (phthalocyaninato)(porphyrinato) rare-earth(III) double-decker complexes upon protonation should be very useful in giving information about the location of the acid proton in the protonated species.

As detailed in the previous report, the molecular structures of both the neutral nonprotonated double-deckers [M^{III}{Pc(α-OC$_5$H$_{11}$)$_4$}(TClPP)] (M=Sm, Eu) and the protonated counterparts [M^{III}H{Pc(α-OC$_5$H$_{11}$)$_4$}(TClPP)] (M=Sm, Eu) were luckily determined simultaneously by X-ray diffraction analyses.[5h] It is worth pointing out again that the location of the acid proton in the protonated double-decker compounds cannot be directly determined on the basis of X-ray diffraction analysis results. However, the experimental structural results reveal that the average M···N$_4$(TClPP) plane distance in [M^{III}H{Pc(α-OC$_5$H$_{11}$)$_4$}(TClPP)] (M=Sm, Eu) is longer, by about 0.029–0.037 Å, than that in [M^{III}{Pc-(α-OC$_5$H$_{11}$)$_4$}(TClPP)] (M=Sm, Eu). In contrast, the average M···N$_4${Pc(α-OC$_5$H$_{11}$)$_4$} plane distance in [Sm^{III}H{Pc(α-OC$_5$H$_{11}$)$_4$}(TClPP)] remains almost the same as in [Sm^{III}{Pc-(α-OC$_5$H$_{11}$)$_4$}(TClPP)] (1.557 Å versus 1.558 Å), while that in [Eu^{III}H{Pc(α-OC$_5$H$_{11}$)$_4$}(TClPP)] is a bit longer (about 0.012 Å) than in [Eu^{III}{Pc(α-OC$_5$H$_{11}$)$_4$}(TClPP)]. Apart from the average M···N$_4$(tetrapyrrole) plane distance, the average dihedral angle φ, which is defined as the average dihedral angle of the individual pyrrole or isoindole rings with respect to the corresponding N$_4$ mean plane, for the TClPP ring is marginally increased by 0.3–0.8°, while that for the Pc(α-OC$_5$H$_{11}$)$_4$ ring is significantly decreased by 1.4–2.3° upon protonation. The fact that more significant distortion takes place in the molecular structure of the porphyrin ligand TClPP upon protonation, while the phthalocyanine side becomes more planar in the double-decker compounds, therefore suggests that the acid proton atom in the mixed protonated (phthalocyaninato)(porphyrinato) rare-earth double-decker complexes should be located on the porphyrin side rather than on the phthalocyanine ring.

Molecular orbitals: Figure 2a shows the orbital energy diagram of [(Pc)Y(Por)]$^-$ together with those of [MgPor] and [MgPc], and Figure 2b compares the calculated molecular orbital energy levels of [(Pc)Y(Por)], [(Pc)Y(Por)]$^-$, [(HPc)Y(Por)], and [(Pc)Y(HPor)], as well as their orbital symmetry. The molecular orbital maps of [(Pc)Y(Por)], [(Pc)Y(Por)]$^-$, [(HPc)Y(Por)], and [(Pc)Y(HPor)] are shown in Figure 3. The calculation results shown in Figures 2a and 3 indicate that the HOMO (218 a$_2$) and HOMO−2 (216 a$_2$) orbitals of [(Pc)Y(Por)]$^-$ are formed from the HOMO−1 (a$_{1u}$) orbital of Por^{2-} and the HOMO (a$_{1u}$) orbital

Figure 2. a) The orbital energy diagram of MgP, [(Pc)Y(Por)]⁻, and MgPc and b) the calculated molecular orbital energy levels of [(Pc)Y(Por)], [(Pc)Y-(Por)]⁻, [(HPc)Y(Por)], and [(Pc)Y(HPor)].

Figure 3. The orbital map of [(Pc)Y(Por)], [(Pc)Y(Por)]⁻, [(HPc)Y(Por)], and [(Pc)Y(HPor)] from the orbital numbers 215 to 222.

of Pc^{2-}, because of their very similar orbital energy. However, the HOMO ($218a_2$) orbital of the reduced double-decker [(Pc)Y(Por)]⁻ is composed of a slightly larger contribution from the HOMO (a_{1u}) of Pc^{2-}, while the HOMO−2 ($216a_2$) orbital has somewhat more content from the HOMO−1 (a_{1u}) orbital of Por^{2-}, due to the slightly higher orbital energy (around 0.06 eV) of the HOMO (a_{1u} orbital) of Pc^{2-} compared to the HOMO−1 (a_{1u} orbital) of Por^{2-}. Taking

the atomic orbital composition on the Pc ring and Por ring as respective for the whole segment, the HOMO and HOMO−2 orbitals of [(Pc)Y(Por)]− can then be considered as the antibonding and bonding orbitals between the Pc and Por rings, respectively. The π–π interaction between the Pc and Por rings in mixed (phthalocyaninato)(porphyrinato) rare-earth complexes can therefore be clearly expressed by the energy difference between the HOMO and HOMO−2 orbitals. However, as clearly shown in Figure 2a, due to the lack of energy-matching of the orbital in Pc^{2-} with the HOMO (a$_{2u}$) of Por^{2-}, the HOMO (a$_{2u}$) of Por^{2-} itself forms the HOMO−1 orbital of [(Pc)Y(Por)]−, with a small contribution from the atomic orbital of yttrium. As also shown in Figure 2a, the LUMO of [MgPor] is 0.74 eV higher in energy than that of [MgPc], as a result, the twofold degenerate LUMO of Pc^{2-} and Por^{2-} form the LUMO and LUMO+1 orbitals, respectively, of [(Pc)Y(Por)]−, almost independently and with a very small degree of contribution from the other ligand. This indicates that the LUMO orbitals of the Pc and Por ligands cannot form "real" molecular orbitals delocalized over both tetrapyrrole rings in [(Pc)Y(Por)]− as in the homoleptic counterpart [Y(Pc)$_2$]−.[8d]

Both the alpha and beta molecular orbitals of [(Pc)Y(Por)] are very similar to those of [(Pc)Y(Por)]− with the same symmetry in terms of atomic composition and appearance, despite the open-shell nature of [(Pc)Y(Por)] (Figure 3). As displayed in Figure 2b, the alpha 218a$_2$ and beta 218a$_2$ orbitals are the highest occupied orbital (HOMO) and lowest unoccupied orbital (LUMO) of [(Pc)Y(Por)], respectively. When neutral [(Pc)Y(Por)] is reduced to [(Pc)Y(Por)]−, the electron should be added into the double-decker molecule and occupy the beta 218a$_2$ orbital. In other words, the hole in neutral double-decker [(Pc)Y(Por)] is localized mainly on the Pc ring due to the fact that the beta 218a$_2$ orbital is contributed to mainly by the Pc ligand (Figure 3). It is worth further noting that the orbitals contributed from the C^1 atoms of the Pc ring and the C^a atoms of the Por ring for both the alpha HOMO−2 orbital (α 216a$_2$) and the beta HOMO−1 orbital (β 216a$_2$) of neutral double-decker [(Pc)Y(Por)] appear to form σ bonding orbitals, while no such bonding orbital is found in the HOMO−2 orbital of the reduced double-decker [(Pc)Y(Por)]− (Figure 3). These results suggest that the interaction between the two tetrapyrrole rings in neutral [(Pc)Y(Por)] is stronger than that in reduced [(Pc)Y(Por)]−, which is consistent with the shorter inter-ring distance in neutral [(Pc)Y(Por)] than in reduced [(Pc)Y(Por)]− (vide supra).

As mentioned above, significant distortion occurs in the molecular structure of mixed (phthalocyaninato)(porphyrinato) yttrium double-decker compounds when the acid proton is attached to one of the tetrapyrrole rings, namely [(HPc)Y(Por)] and [(Pc)Y(HPor)]. However, the frontier molecular orbitals of [(HPc)Y(Por)] are very similar to those of [(Pc)Y(Por)]− in appearance, as shown in Figure 3, indicating that the relative order of orbital energy of Pc and Por ligands in [(HPc)Y(Por)] does not change in comparison with that in [(Pc)Y(Por)]−. It must be pointed out that the

energy difference between corresponding orbitals of the Por and Pc rings in [(HPc)Y(Por)] becomes larger than in [(Pc)Y(Por)]− as a result of the shorter distance between yttrium and the Por ring, and longer distance between yttrium and the Pc ring in [(HPc)Y(Por)] due to the repulsion between the proton attached onto the Pc ring and the yttrium. This is illustrated well by the increased energy difference between the LUMO (219a orbital) and the 222a orbital in [(HPc)Y(Por)] (0.75 eV) relative to that between the LUMO and LUMO+1 in [(Pc)Y(Por)]− (0.51 eV). Along with changing the acid proton from the Pc ring in [(HPc)Y-(Por)] onto the Por ring in [(Pc)Y(HPor)], a large change is observed in the orbital energies of the mixed (phthaloycani-nato)(porphyrinato) yttrium double-decker complex, resulting in a significant difference in the orbitals of [(Pc)Y-(HPor)] from those of [(HPc)Y(Por)], [(Pc)Y(Por)], and [(Pc)Y(Por)]− (Figures 2 and 3). The HOMO of [(Pc)Y-(HPor)] is mainly distributed on the Pc ring, whereas the HOMO−1 and HOMO−2 orbitals are mainly on the Por ring. The approximately degenerate LUMO (219) and 220 orbitals, as well as the other two approximately degenerate 221 and 222 orbitals of [(Pc)Y(HPor)], with an approximate C_s molecular symmetry, are delocalized over both the Pc and Por ligands. In contrast to the situation in [(HPc)Y-(Por)], repulsion between the acid proton and yttrium in [(Pc)Y(HPor)] pushes the yttrium farther from the Por ring but closer to the Pc ring. This leads to a decrease in the orbital energy level of the Por ligand and an increase in the orbital energy level of the Pc ligand in this protonated species. As a result, the HOMO of the Pc ligand with a much higher energy relative to that of the Por ligand, and the HOMO of the Por ligand almost independently form the HOMO and HOMO−1 orbitals of [(Pc)Y(HPor)], respectively. In other words, there exists almost no interaction between the frontier occupied orbitals of the Pc and Por rings in [(Pc)Y-(HPor)]. However, the increase in energy of the LUMO for the Pc ligand together with the decrease of the LUMO for the Por ligand in [(Pc)Y(HPor)] due to the repulsion between the acid proton attached to the Por ring and the yttrium makes the LUMOs of the two tetrapyrrole (Pc and Por) ligands match well in terms of orbital energy, resulting in a strong interaction between the LUMO orbitals of the Pc and Por ligands. It is worth noting that the formation of "real" molecular orbitals delocalized over both tetrapyrrole rings between the LUMO of the Pc and Por ligands would increase the stability of the species [(Pc)Y(HPor)] over [(HPc)Y(Por)], in which the LUMO of the Pc and Por ligands independently form the LUMO and LUMO+1 molecular orbitals. Further support for this point comes from the approximately 3 kcal mol^{-1} lower total electronic energy of [(Pc)Y(HPor)] in comparison with that of [(HPc)Y(Por)] according to our calculation results. All these results suggest that the acid proton in the protonated mixed (phthalocyani-nato)(porphyrinato) yttrium compound should localize on the Por ring rather than the Pc ring.

Atomic charges: Table 1 lists the atomic charges of [(Pc)Y-(Por)], [(Pc)Y(Por)]⁻, [(HPc)Y(Por)], and [(Pc)Y(HPor)], calculated by a full natural bond orbital (NBO) analysis population method. When [(Pc)Y(Por)] is reduced to [(Pc)Y(Por)]⁻, the negative charges on C^3, C^4, and C^b increase by 0.015, 0.021, and 0.013 e, respectively, while the positive charges on C^1 and C^a decrease by 0.041 and 0.014 e, respectively. This agrees well with the conclusion derived from the orbital analysis that the added electron will occupy the beta a_2 orbital (LUMO) of the neutral [(Pc)Y(Por)], which is mainly composed of the p_z orbitals of the C^1, C^3, and C^4 atoms of the Pc ligand, and C^a and C^b atoms of the Por ligand. The positive charge on the yttrium atom increases from +2.079 e in [(Pc)Y(Por)] to +2.085 e in [(Pc)Y-(Por)]⁻, revealing the weakening of the coordination bonds between yttrium and pyrrole as well as isoindole nitrogen atoms. This is in line with the increase in the Y···N^1 and Y···N^a bond lengths, along with the reduction of [(Pc)Y-(Por)] to [(Pc)Y(Por)]⁻, vide supra. Our calculation results also reveal that along with the reduction of neutral species, the negative charge distributed on the Pc and Por rings increases from −0.867 and −1.212 e in [(Pc)Y(Por)] to −1.581 and −1.504 e in [(Pc)Y(Por)]⁻, respectively. The more significant change of negative charge in the Pc ring in comparison with that in the Por ring in the double-decker molecule along with the reduction gives further support for the point that the hole in neutral [(Pc)Y(Por)] should be localized mainly on the Pc ring.

With respect to [(Pc)Y(Por)], incorporation of one hydrogen atom on the Pc ring increases both the positive charge on yttrium (from +2.079 to +2.12 e) and negative charge on the Pc and Por ligands (from −0.867 and −1.212 e to −1.15 and −1.44 e, respectively) due to the repulsion between the acid proton attached to the Pc ligand and the yttrium. In addition, the acid proton connected to N^{1A} of the Pc ring in [(HPc)Y(Por)] has a positive charge of +0.47 e. Contrary to [(HPc)Y(Por)], incorporation of an acid proton on the Por ring induces a decrease in the negative charge on the Por ligand to −1.07 e, despite the increase in the positive charge on yttrium and negative charge on the Pc ring to +2.10 and −1.49 e, respectively, because of the repulsion be-

tween the acid proton connected to the Por ring and the yttrium. The positive charge on the acid proton in [(Pc)Y-(HPor)] is found to be +0.46 e, slightly smaller than in [(HPc)Y(Por)]. According to Coulomb's law, the electrostatic repulsion between yttrium and the acid proton in [(Pc)Y-(HPor)] is smaller than in [(HPc)Y(Por)], indicating that [(Pc)Y(HPor)] is a more stable protonated species than [(HPc)Y(Por)]. Furthermore, on the basis of negative charge distribution analysis, [(Pc)Y(HPor)] can be recognized as a more stable structure than [(HPc)Y(Por)] as a similar amount of negative charge can be distributed over a larger conjugated system of Pc in the former species than over a smaller conjugated system of Por in the latter species. In line with the previous point, the results obtained in this section also suggest that acid proton in the protonated mixed (phthalocyaninato)(porphyrinato) yttrium compound should be localized on the Por ring rather than the Pc ring.

Electronic absorption spectra: Figure 4 compares the simulated electronic absorption spectra of [(Pc)Y(Por)] and
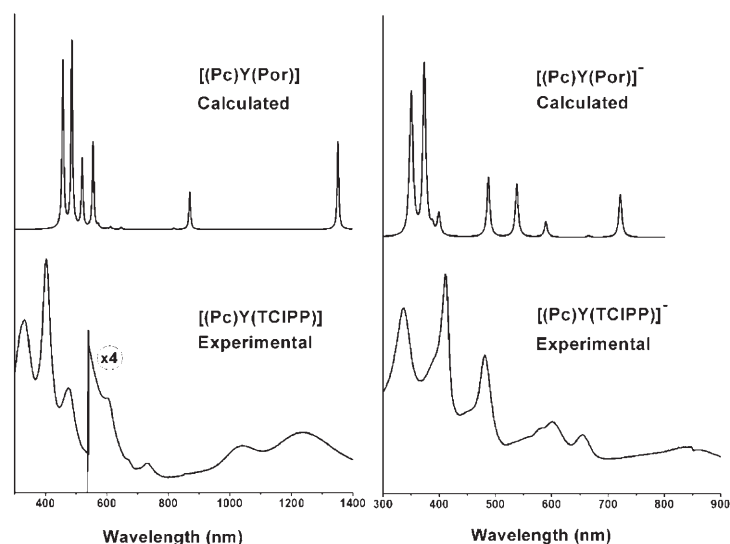

Figure 4. Simulated electronic absorption spectra of [(Pc)Y(Por)] and [(Pc)Y(Por)]⁻ and experimental absorption spectra of [(Pc)Y(TClPP)] and [(Pc)Y(TClPP)]⁻ in CHCl₃.

Table 1. Calculated NBO charges of [(Pc)Y(Por)], [(Pc)Y(Por)]⁻, [(HPc)Y(Por)], and [(Pc)Y(HPor)].

Atom[a]	[(Pc)Y(Por)]	[(Pc)Y(Por)]⁻	[(HPc)Y(Por)]				[(Pc)Y(HPor)]			
			A	B	C	D	A	B	C	D
Y(+)	2.079	2.085	2.120				2.100			
N^1(−)	0.687	0.681	0.647	0.714	0.713	0.714	0.739	0.739	0.739	0.739
N^2(−)	0.539	0.538	0.524	0.528	0.528	0.524	0.536	0.529	0.528	0.529
C^1(+)	0.498	0.457	0.462	0.469/0.462	0.479	0.462/0.469	0.457/0.463	0.463/0.457	0.465/0.462	0.462/0.465
C^2(−)	0.070	0.065	0.067	0.067/0.073	0.069	0.073/0.067	0.071/0.070	0.070/0.071	0.070	0.070
C^3(−)	0.174	0.189	0.179	0.179/0.180	0.179	0.180/0.179	0.186/0.182	0.182/0.186	0.182/0.184	0.184/0.182
C^4(−)	0.205	0.226	0.206	0.207/0.208	0.207	0.208/0.207	0.211	0.211	0.211	0.211
N^a(−)	0.702	0.692	0.744	0.744	0.744	0.744	0.643	0.711	0.701	0.710
C^m(−)	0.230	0.227	0.221	0.218	0.221	0.229	0.235	0.203	0.203	0.235
C^a(+)	0.200	0.186	0.188/0.186	0.190/0.189	0.189/0.190	0.186/0.188	0.191	0.190/0.194	0.193	0.194/0.190
C^b(−)	0.224	0.237	0.223/0.227	0.224/0.225	0.225/0.224	0.227/0.223	0.206	0.213/0.225	0.220	0.225/0.213
Pc(−)	0.867	1.581	1.15				1.49			
Por(−)	1.212	1.504	1.44				1.07			

[a] The sign in parentheses is the sign of the charge distributed on the corresponding atom or ligand; see Figure 1 for atom labeling.

[(Pc)Y(Por)]⁻ with the experimental spectra of [(Pc)Y-(TClPP)] and [(Pc)Y(TClPP)]⁻.[7i] Table 2 summarizes the electronic transitions of the main absorption bands. The simulated electronic absorption spectra of [(Pc)Y(Por)] and [(Pc)Y(Por)]⁻ correspond well with the experimental ones of [(Pc)Y(TClPP)] and [(Pc)Y(TClPP)]⁻ for most absorption bands. As expected, [(Pc)Y(Por)] shows a different electronic absorption spectrum from its reduced species [(Pc)Y(Por)]⁻, due to its open-shell nature. The calculated band at 457 nm for [(Pc)Y(Por)] is mainly due to the electronic transition from alpha HOMO−2 ($216a_2$ orbital) to alpha LUMO+1 ($221e*$ and $222e*$ orbitals), and can be assigned as the Soret band of the Por ligand on the basis of orbital distribution analysis, which corresponds with the experimental absorption at 401 nm for [(Pc)Y(TClPP)].[7i] The bands at 486 and 520 nm for [(Pc)Y(Por)] are mainly due to the electronic transitions from the beta degenerate 205 and 206 orbitals to the beta LUMO ($218a_2*$, the hole orbital), which have significant Pc character according to the contribution analysis of the 205, 206, and 218 orbitals. The band at 486 nm might correspond with the experimental absorption observed at 470 nm for [(Pc)Y(TClPP)].[7i] Despite the absence of observation of the corresponding absorption for the band at 520 nm in the experimental spectrum of [(Pc)Y-(TClPP)];[7i] this finds a counterpart at 538 nm in the spectrum of [Y{Pc(α-OC$_5$H$_{11}$)$_4$}(TClPP)].[5h] This is also true for the calculated band at 555 nm of [(Pc)Y(Por)], which corresponds with the experimental absorption at 590 nm for [Y{Pc(α-OC$_5$H$_{11}$)$_4$}(TClPP)].[5h] Due to its electronic transition nature from the alpha and beta $216a_2$ orbitals to the corresponding alpha and beta degenerate $219e*$ and $220e*$ orbitals, this band at 555 nm is assigned as the Q-band for the neutral double-decker compound. Similarly, the very weak bands calculated at 572 and 613 nm are also assigned

as the Q-bands of [(Pc)Y(Por)] according to their electronic transition nature, which are believed to also contribute to the observed absorptions of the corresponding neutral mixed (phthalocyaninato)(porphyrinato) rare-earth complexes in the same region. The fourth calculated Q-band for [(Pc)Y(Por)] appears at 870 nm, which is mainly due to the electronic transition from the alpha HOMO ($218a_2$) to the alpha LUMO ($219e*$ and $220e*$). Orbital distribution analysis shows that this transition induces the electrons that delocalize over both the Pc and Por ligands in the double-decker molecule to concentrate onto the phthalocyanine moiety. This band corresponds to the experimental absorption at 732 nm for [(Pc)Y(TClPP)].[7i] It is worth noting that a similar band also appears in the simulated absorption spectra of [(Pc)Y(Por)]⁻, [(HPc)Y(Por)], and [(Pc)Y(HPor)] at 722, 753 (774), and 799 (814) nm, respectively. According to our TDDFT calculations, the band at 1353 nm for [(Pc)Y-(Por)] with medium intensity, which corresponds with the experimental absorption at 1238 nm for [(Pc)Y(TClPP)],[7i] is due to the electronic transition from the bonding beta HOMO−1 ($216a_2$) orbital to the antibonding beta LUMO ($218a_2*$) (Table 2). As described above, due to the main contribution from the Por and Pc ligands to the beta HOMO−1 ($216a_2$) and beta LUMO ($218a_2$) orbitals, respectively, this band can therefore be attributed to the electron transfer from the Por ligand to the Pc ring in the neutral double-decker. This assignment is additionally supported by the ground-to-excited-state transition electric dipole moment of about 0.09 au along the z axis. As mentioned in the above molecular orbital section, the energy difference between the $216a_2$ and $218a_2$ orbitals in the mixed (phthalocyaninato)(porphyrinato) yttrium compound [(Pc)Y(Por)] is a good indication of the π–π interaction between the Pc and Por rings. This band therefore forms the most characteristic

Table 2. Calculated electronic absorption spectroscopic data for [(Pc)Y(Por)], [(Pc)Y(Por)]⁻, [(HPc)Y(Por)], and [(Pc)Y(HPor)].

λ[a]	[(Pc)Y(Por)] Transitions[b]	λ[a]	[(Pc)Y(Por)]⁻ Transitions[b]	λ[a]	[(HPc)Y(Por)] Transitions[b]	λ[a]	[(Pc)Y(HPor)] Transitions[b]
		351	18% $215a_1{\rightarrow}221e*$ 15% $218^{HOMO}a_2{\rightarrow}227e*$	355	25% $206a{\rightarrow}219^{LUMO}a*$ 24% $207a{\rightarrow}220^{LUMO'}a*$	366	29% $209a{\rightarrow}219^{LUMO}a*$ 26% $214a{\rightarrow}222a*$
		373	21% $215a_1{\rightarrow}221e*$ 13% $216a{\rightarrow}222a*$	371	33% $208a{\rightarrow}220^{LUMO'}a*$ 16% $216a_2{\rightarrow}222e*$	385	17% $212a{\rightarrow}220^{LUMO'}a*$ 26% $216a{\rightarrow}221a*$
		399	20% $215a_1{\rightarrow}220^{LUMO}e*$ 15% $215a_1{\rightarrow}229a_2*$	414	35% $214a{\rightarrow}219^{LUMO}a*$ 31% $212a{\rightarrow}219^{LUMO}a*$	405	59% $215a{\rightarrow}219^{LUMO}a*$
457	30% $216a_2{\rightarrow}221e*(\alpha)$	487	19% $216a_2{\rightarrow}221e*$ 17% $217a_1{\rightarrow}222e*$	491	46% $216a{\rightarrow}221a*$ (41% $216a{\rightarrow}222a*$)	465	45% $216a{\rightarrow}222a*$ (47% $216a{\rightarrow}221a*$)
486	14% $205e{\rightarrow}218^{LUMO}a_2*(\beta)$ 12% $216a_2{\rightarrow}222e*(\beta)$					505	53% $217a{\rightarrow}221a*$ (50% $217a{\rightarrow}222a*$)
520	28% $206e{\rightarrow}218^{LUMO}a_2*(\beta)$						
555	20% $216a_2{\rightarrow}219e*(\beta)$ 19% $216a_2{\rightarrow}220^{LUMO}e*(\alpha)$	538	34% $216a_2{\rightarrow}220^{LUMO}e*$ 24% $216a_2{\rightarrow}219^{LUMO}e*$	583 595	51% $216a{\rightarrow}220^{LUMO'}a*$ 52% $216a{\rightarrow}219^{LUMO}a*$	546 556	55% $217a{\rightarrow}220^{LUMO'}a*$ 53% $217a{\rightarrow}219^{LUMO}a*$
572	19% $218^{HOMO}a_2{\rightarrow}221e*(\alpha)$ 15% $218^{HOMO}a_2{\rightarrow}222e*(\alpha)$	589	33% $218^{HOMO}a_2{\rightarrow}222e*$ 26% $218^{HOMO}a_2{\rightarrow}221e*$	563	55% $218^{HOMO}a{\rightarrow}221a*$ (47% $218^{HOMO}a{\rightarrow}222a*$)	620	51% $218^{HOMO}a{\rightarrow}221a*$
613	13% $217a_1{\rightarrow}219^{LUMO}e*(\beta)$ 13% $217a_1{\rightarrow}220^{LUMO}e*(\beta)$	666	70% $217a_1{\rightarrow}220^{LUMO}e*$ 30% $217a_1{\rightarrow}219^{LUMO}e*$	735	61% $217a{\rightarrow}219^{LUMO}a*$		
870	52% $218^{HOMO}a_2{\rightarrow}220^{LUMO}e*$ (α)	722	43% $218^{HOMO}a_2{\rightarrow}219^{LUMO}e*$ 36% $218^{HOMO}a_2{\rightarrow}220^{LUMO}e*$	753 774	51% $218^{HOMO}a{\rightarrow}220^{LUMO'}a*$ 70% $218^{HOMO}a{\rightarrow}219^{LUMO}a*$	799 814	72% $218^{HOMO}a{\rightarrow}220^{LUMO'}a*$ 74% $218^{HOMO}a{\rightarrow}219^{LUMO}a*$
1353	$216a_2{\rightarrow}218^{LUMO}a_2*$ (β)						

[a] Calculated wavelength in nm. [b] The contributions of each electronic transitions to the absorption band shown in percent have been normalized.

band for the neutral mixed (phthalocyaninato)(porphyrinato) yttrium double-decker compound. In line with this result, systematic studies on the electronic absorption spectra of [(Pc)M(TClPP)] (M = Y, La→Lu, except Ce and Pm) reveal that the absorption in the range of 1148–1418 nm is sensitive to the ionic radius of the metal center.[7i] Along with the decrease of the central rare-earth ionic size, a blue shift is observed for this absorption, indicating the enhanced π–π interaction between the Pc and Por rings in the same order. At the end of this paragraph, it is worth noting that the Soret band of phthalocyanine is not detected by our TDDFT calculations, suggesting the absence of a Pc^{2-} ligand in [(Pc)Y(Por)]. However, the Soret absorption of phthalocyanine was observed at 332 nm despite its relatively weak intensity in comparison with the Soret band of the Por ligand in [(Pc)Y(TClPP)].[7i] This appears strange but can be reasonably rationalized by the possible existence of Pc^{2-} for a short time due to the electron transfer from the Por ligand to the Pc ring in [(Pc)Y(TClPP)]. On the basis of these calculation results, the absence of the phthalocyanine Soret band, together with the appearance of the bands with significant phthalocyanine character involving the semi-occupied molecular orbital (SOMO) at 486, 520, and 1353 nm for [(Pc)Y(Por)], indicate that the hole should localize on the Pc ring in the neutral mixed (phthalocyaninato)(porphyrinato) yttrium double-decker compound.

Along with the reduction of neutral [(Pc)Y(Por)] to [(Pc)Y(Por)]−, the absorption bands at 486, 520, and 1353 nm for [(Pc)Y(Por)] disappear due to the re-pairing of alpha and beta orbitals and the disappearance of the hole on the Pc ring in [(Pc)Y(Por)]− (Figure 4). This gives further support to our assignments of the bands at 486, 520, and 1353 nm for [(Pc)Y(Por)] as transitions involving the semi-occupied orbital (beta $218a_2$*). In contrast, three new bands appear at 351, 373, and 399 nm in the simulated absorption spectrum of [(Pc)Y(Por)]−. The bands at 351 and 399 nm might correspond with the bands of [(Pc)Y(TClPP)]− at 337 and 411 nm, respectively, which are assigned as the Soret bands of phthalocyanine and porphyrin, respectively (Figure 4 and Table 2). Due to the similar electronic transition nature between the two bands at 351 and 373 nm, mainly from $215a_1$ to $221e$* and $222e$* orbitals, the calculated band at 373 nm is also believed to contribute to the observed Soret band of phthalocyanine at 337 nm for [(Pc)Y-(TClPP)]−. The bands appearing at 487, 538, and 722 nm for [(Pc)Y(Por)]− correspond with the experimental absorptions at 481, 581, and 848 nm for [(Pc)Y(TClPP)]−, which can be assigned as the Soret band of Por and the first and fourth Q-bands for the reduced double-decker, in terms of their electronic transition nature. The weak band at 589 nm for [(Pc)Y(Por)]− due to the electronic transition from HOMO ($218a_2$) to LUMO+1 ($221e$* and $222e$* orbitals) is the second Q-band of [(Pc)Y(Por)]−, which corresponds to the observed absorption at 601 nm for [(Pc)Y(TClPP)]− (Figure 4). The third Q-band for [(Pc)Y(Por)]− with very weak intensity calculated at 666 nm is interesting. This is mainly due to the electronic transition from the $217a_1$ orbi-

tal (HOMO−1) to $219e$* and $220e$* orbitals (LUMO). The electric dipole moments for this transition are in the xy plane. However, orbital contribution analyses show that the $217a_1$ orbital is mainly formed from the Por ligand with a small contribution from the atomic orbital of yttrium, while the $219e$* and $220e$* orbitals are mainly distributed on the Pc moiety with very little contribution from the Por ligand. In terms of the final transition result that this band actually leads to electron transfer from the Por to Pc ligand in [(Pc)Y(Por)]−, it can therefore be assigned as a charge-transfer-type transition. This band corresponds with the experimental absorption at 654 nm for [(Pc)Y(TClPP)]−. As a result, both the appearance of the phthalocyanine Soret band and disappearance of the characteristic phthalocyanine π-radical anion bands in the reduced double-decker species [(Pc)Y(Por)]− give further support for the localization of the hole on the Pc ring in the neutral double-decker species [(Pc)Y(Por)].

Figure 5 compares the simulated electronic absorption spectra of [(HPc)Y(Por)] and [(Pc)Y(HPor)]. As expected, both [(HPc)Y(Por)] and [(Pc)Y(HPor)] show similar elec-
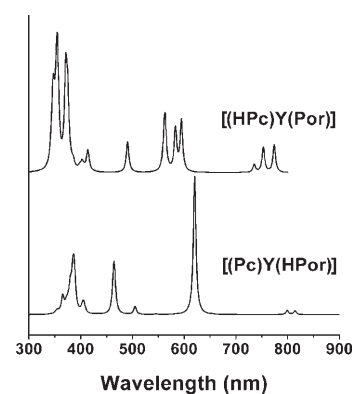

Figure 5. Simulated electronic absorption spectra of [(HPc)Y(Por)] and [(Pc)Y(HPor)].

tronic absorption spectroscopic features to [(Pc)Y(Por)]− due to their similar electronic structure. However, the decrease in molecular symmetry from C_{4v} for [(Pc)Y(Por)]− to approximate C_s for [(HPc)Y(Por)] leads to the splitting of some bands in the absorption spectrum of the protonated double-decker compounds. For example, the Q-band of [(Pc)Y(Por)]− at 538 nm is split into two bands at 583 and 595 nm for [(HPc)Y(Por)] due to the small energy difference between orbitals 219 and 220, while the one at 589 nm for [(Pc)Y(Por)]− remains not split at 563 nm for [(HPc)Y-(Por)]. It is seen that the two Q-bands for [(Pc)Y(Por)]− due to electronic transitions from HOMO−2 to LUMO and from HOMO to LUMO+1, respectively, are reversed in energy compared to the corresponding bands of [(HPc)Y-(Por)], due to the increase in the orbital energy gap between LUMO and LUMO+1 and the decrease in the orbital

energy gap between HOMO and HOMO−2 induced by the repulsion between the proton attached to the Pc ring and yttrium atoms (molecular orbitals section, Figure 2b).

Despite the similar molecular electronic structure and similar electronic absorption spectrum, the nature of the bands for [(Pc)Y(HPor)] is quite different from that for [(HPc)Y(Por)] due to the different orbital distribution. For example, the electronic transitions from HOMO to LUMO of [(HPc)Y(Por)], which give absorption bands at 753 and 774 nm (Figure 5), result in the localization of electrons that are delocalized over both the Pc and Por ligands on the phthalocyanine moiety. In contrast, the electronic transitions giving absorption bands at 799 and 814 nm for [(Pc)Y-(HPor)] result in the delocalization of electrons that are almost localized on the Pc ring over both the Pc and Por rings. The two bands at 366 and 385 nm for [(Pc)Y(HPor)] can be assigned as the Soret bands of the Pc ligand according to the contribution analysis of the orbitals involved in these electronic transitions, which correspond to the calculated bands at 351 and 373 nm of [(Pc)Y(Por)]⁻. The Soret bands of Por in [(Pc)Y(HPor)] appearing at 405 and 465 nm correspond with the bands at 399 and 487 nm for [(Pc)Y-(Por)]⁻, respectively. The weak band at 505 nm for [(Pc)Y-(HPor)] is due to the electronic transition from 217 (HOMO−1) to 221 and 222 orbitals (LUMO+1). Due to the fact that the 217 orbital is almost localized on the Por ring, while the 221 and 222 orbitals are delocalized over both the Pc and Por rings, this band can be assigned as an electron rearrangement band. It must be pointed out that no corresponding band is found in the simulated spectra of [(Pc)Y(Por)]⁻ and [(HPc)Y(Por)], indicating that this band is characteristic of the protonated species [(Pc)Y(HPor)]. The strong Q-band of [(Pc)Y(HPor)] at 620 nm corresponds to the Q-band of [(Pc)Y(Por)]⁻ at 589 nm, whereas the two very weak Q-bands of [(Pc)Y(HPor)] at 546 and 556 nm correspond to the strong Q-band of [(Pc)Y(Por)]⁻ at 538 nm. The two bands at 799 and 814 nm due to electronic transitions from HOMO to LUMO for [(Pc)Y(HPor)] correspond with the band at 722 nm for [[(Pc)Y(Por)]⁻.

Comparison between the calculated spectroscopic results for [(HPc)Y(Por)] and [(Pc)Y(HPor)], and in particular with experimental data for [YH{Pc(α-OC₅H₁₁)₄}(TClPP)],[5h] reveals that the simulated spectrum of [(Pc)Y(HPor)] seems to correspond better with the experimental spectrum of [YH{Pc(α-OC₅H₁₁)₄}(TClPP)] than [(HPc)Y(Por)]. Especially, the characteristic weak band of [(Pc)Y(HPor)] at 505 nm, which is absent in the spectrum of [(HPc)Y(Por)], corresponds well with the observed absorption at 490 nm for [YH{Pc(α-OC₅H₁₁)₄}(TClPP)]. These results provide additional support to the point that the acid proton should be localized on the Por ring instead of the Pc ring in the protonated mixed (phthalocyaninato)(porphyrinato) yttrium complex.

Infrared spectra: The simulated infrared spectra of [(Pc)Y-(Por)], [(Pc)Y(Por)]⁻, [(HPc)Y(Por)], and [(Pc)Y(HPor)] are shown in Figure S1, Supporting Information. The infrared spectrum of [(Pc)Y(Por)]⁻ shows typical characteristic absorptions of the phthalocyanine dianion Pc²⁻ at 1341, 1094, and 1048 cm⁻¹, and of the porphyrin dianion Por²⁻ at 946 cm⁻¹.[8d, 14] In contrast, the typical characteristic bands of Pc²⁻ disappear or lose intensity in the spectrum of [(Pc)Y-(Por)], while those in the spectrum of Por²⁻ gain intensity. However, one new, strong peak due to Y···N¹ stretching mixed with Pc stretching appearing at 1257 cm⁻¹ in the IR spectrum of [(Pc)Y(Por)] seems to be the characteristic absorption IR band of the phthalocyanine monoanion radical Pc·⁻ according to our calculations. These results suggest that the hole in neutral [(Pc)Y(Por)] should be localized on the Pc ring rather than on the Por ring. Nevertheless, weak bands which involve the acid proton are observed at 3388 and 3389 cm⁻¹, respectively, in the simulated IR spectra of [(HPc)Y(Por)] and [(Pc)Y(HPor)].

The location of the hole in the neutral nonprotonated mixed (phthalocyaninato)(porphyrinato) yttrium(III) complex: As stated in the previous sections, the IR spectroscopic results on the absorption spectra of neutral non-protonated mixed (phthalocyaninato)(porphyrinato) rare-earth(III) complexes have verified the location of the hole on the Pc ring.[5a–c, 7i] However, there seems to be no further evidence to support this point. The present work on the structures, molecular orbitals, atomic charges, and electronic absorption spectra of [(Pc)Y(Por)] and [(Pc)Y(Por)]⁻ studied by DFT method renders it possible to clarify the location of hole in neutral nonprotonated mixed (phthalocyaninato)(porphyrinato) rare-earth(III) complexes. Along with the reduction of [(Pc)Y(Por)] to [(Pc)Y(Por)]⁻, it has been found that more change occurs in the structure of the Pc ring than the Por ring, indicating the added electron has more influence on the Pc ring than the Por ring in [(Pc)Y(Por)]. Molecular orbital analysis reveals that the hole locates in the orbital of beta 218a₂ in [(Pc)Y(Por)], which has more content from the orbital of the Pc ligand. The study on the atomic charge distribution indicates that more than 70% of the negative charge is introduced onto the Pc ring when [(Pc)Y(Por)] is reduced to [(Pc)Y(Por)]⁻. The characteristic electronic absorption band of [(Pc)Y(Por)] at 1353 nm due to the electronic transition from beta HOMO−1 to beta LUMO is assigned as electron transfer from the Por to the Pc ring to fill the hole on the Pc ring. Moreover, the calculated electronic absorption spectroscopic results show that no Soret band of Pc ring exists in the spectrum of [(Pc)Y(Por)], and the characteristic π-radical anion bands involving the semi-occupied molecular orbital (SOMO) at 486, 520, and 1353 nm have significant Pc character. The IR theoretical result that the Pc²⁻ marker bands get weaker, the Por²⁻ marker band becomes stronger, and a new Pc·⁻ marker absorption appears in the simulated spectrum of neutral [(Pc)Y(Por)] in comparison with that of [(Pc)Y(Por)]⁻, confirms the experimental finding that the hole localizes on the Pc ring in [(Pc)Y-(Por)] on the basis of the IR spectroscopic technique. In conclusion, all the calculated results suggest that the hole should localize on the Pc ring in the neutral non-protonated

mixed (phthalocyaninato)(porphyrinato) yttrium(III) compound.

The location of the acid proton in the protonated mixed (phthalocyaninato)(porphyrinato) yttrium(III) complex: The location of the acid proton in the protonated mixed (phthalocyaninato)(porphyrinato) rare-earth(III) complex has been puzzling scientists in this field for a long time due to the failure of single-crystal X-ray diffraction anaysis, ^{1}H NMR, and absorption spectroscopic methods to determine the location of this proton. However, on the basis that the hole is probably localized on the Pc ring in the neutral mixed (phthalocyaninato)(porphyrinato) rare-earth(III) complex, it has been supposed that the acid proton in the mixed protonated (phthalocyaninato)(porphyrinato) rare-earth(III) compound should localize on the Pc ring rather than the Por ring.[5h]

According to the present calculation results, the protonated double-decker with an acid proton attached on the Por ligand in the form of [(Pc)Y(HPor)] is more stable than [(HPc)Y(Por)] in terms of molecular electronic energy. The trend revealed by comparing the single-crystal molecular structures of protonated mixed (phthalocyaninato)(porphyrinato) rare-earth(III) complexes with corresponding neutral nonprotonated counterparts[5h] corresponds well with that obtained by comparing the calculated molecular structures of [(Pc)Y(HPor)] and [(Pc)Y(Por)]. Calculations on the molecular orbitals of different species of mixed (phthalocyaninato)(porphyrinato) yttrium(III) double-decker complexes reveal the stronger orbital interaction between the Pc ring and the Por ligand in the LUMO and LUMO+1 orbitals of [(Pc)Y(HPor)] over [(HPc)Y(Por)], indicating that the former species is the more stable. This point is additionally supported by the atomic charge calculation results on [(Pc)Y(HPor)] and [(HPc)Y(Por)]. Furthermore, the calculated absorption spectrum of [(Pc)Y(HPor)] appears to correspond better with the experimental one of [YH{Pc(α-OC$_5$H$_{11}$)$_4$}(TClPP)] than [(HPc)Y(Por)]. In particular, the characteristic weak band of [(Pc)Y(HPor)] at 505 nm, which is absent in the spectrum of [(HPc)Y(Por)], corresponds well with the observed absorption at 490 nm for [YH{Pc(α-OC$_5$H$_{11}$)$_4$}(TClPP)].[5h] In conclusion, all the data from analyses of energy, molecular structures, molecular orbitals, atomic charge distribution, and electronic absorption spectra of different species of mixed (phthalocyaninato)(porphyrinato) yttrium(III) compounds indicate that the acid proton in protonated mixed (phthalocyaninato)(porphyrinato) rare-earth(III) complexes should localize on the Por ring rather than the Pc ligand.

To obtain more information about the location of acid proton, another two possible protonated species of double-decker {[(H)(Pc)Y(Por)] and [(Pc)Y(Por)(H)]}, in which the acid proton locates at the center of the four isoindole or pyrrole nitrogen atoms of the Pc or Por ring, respectively, (Figure S2, Supporting Information), have also been studied. However, calculation results reveal two degenerate imaginary frequencies due to the acid proton vibrating towards the

nitrogen atoms for both [(H)(Pc)Y(Por)] and [(Pc)Y-(Por)(H)], therefore completely excluding the possibility of these two forms of protonated species of double-decker compound. In addition, the calculated distance from the acid proton to the isoindole or pyrrole nitrogen atom in [(H)(Pc)Y(Por)] or [(Pc)Y(Por)(H)] is larger than 2.0 Å, significantly larger than the common H−N covalent bond length (about 1.01 Å).

It is worth noting that electron transfer from the Por ring to the Pc ring in neutral [(Pc)Y(Por)] is necessary for the acid proton to be introduced onto the Por ring to form [(Pc)Y(HPor)]. Scheme 1 describes the possible process for
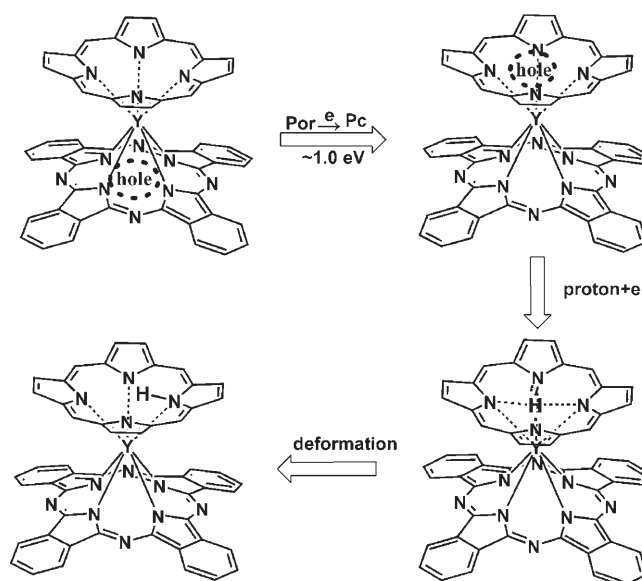
Scheme 1. Formation of [(Pc)Y(HPor)] from [(Pc)Y(Por)].

the formation of [(Pc)Y(HPor)] from [(Pc)Y(Por)]. Firstly, electron transfer from the Por ring to the Pc ring takes place, resulting in a double-decker species with the hole on the Por ring. The energy barrier for this electron-transfer process is not high because of the small beta HOMO–LUMO gap of [(Pc)Y(Por)]. The observation of the phthalocyanine Soret band in neutral mixed (phthalocyaninato)-(porphyrinato) rare-earth complexes proves the formation of Pc^{2-} due to such an electron-transfer process. Secondly, when one hydrogen atom (actually a proton and an electron) gets close enough to the Por ring of the resulting double-decker species, the electron will fill the hole on the Por ring and the proton will form a N−H covalent bond with one or all of the four pyrrole nitrogen atoms on the Por ligand, yielding a primal protonated double-decker species, which undergoes some structural deformation to form the final protonated double-decker compound [(Pc)Y-(HPor)]. However, the hydrogen atom can also directly attach onto the Pc ring of neutral [(Pc)Y(Por)] to form the protonated species [(HPc)Y(Por)]. Due to the higher electronic energy of [(HPc)Y(Por)] than [(Pc)Y(HPor)] and

FULL PAPER

some possible electron transfer modes between the Pc ring and Por ring in [(HPc)Y(Por)], [(HPc)Y(Por)] will finally transform into the more thermodynamically stable species [(Pc)Y(HPor)], despite the fact that the detailed mechanism for this process is not clear at this stage.

Conclusion

On the basis of comparative studies of the molecular structures, molecular orbitals, atomic charges, electronic absorption spectra, and infrared spectra of [(Pc)Y(Por)], [(Pc)Y-(Por)]$^-$, [(HPc)Y(Por)], and [(Pc)Y(HPor)] by the DFT method, the hole in neutral nonprotonated mixed (phthalocyaninato)(porphyrinato) rare-earth(III) complexes is confirmed to localize on the Pc ring. This is in line with the experimental findings using IR technology. However, contrary to the previously expected point, comparative theoretical results indicate that the acid proton in protonated mixed (phthalocyaninato)(porphyrinato) rare-earth(III) complexes prefers to localize on the Por ring rather than the Pc ring.

Experimental Section

Computational details: The primal input structure of [(Pc)Y(Por)] was obtained by putting the yttrium atom in the center of parallel phthalocyanine (Pc) and porphyrin (Por) rings, in which the distance between the Pc and Por rings was set to 3.0 Å and the Pc ring was rotated 45° round the axis passing through the rare earth atom and perpendicular to the Pc and Por rings. The primal input structure of [(Pc)Y(Por)]$^-$ was the same as for [(Pc)Y(Por)]. For the protonated species [(HPc)Y(Por)] and [(Pc)Y(HPor)], protons were added to one of the isoindole or pyrrole nitrogen atoms of the Pc or Por ring, respectively. In [(H)(Pc)Y(Por)] and [(Pc)Y(Por)(H)], the proton was added to the center of four isoindole or pyrrole nitrogen atoms of the Pc or Por ring, respectively, and the C_{4v} symmetry was kept. The hybrid density functional B3LYP (Becke–Lee–Young–Parr composite of exchange-correlation functional) method was used for both geometry optimizations and property calculations.[12] In all cases, the LANL2DZ basis set was used.[13] The Berny algorithm using redundant internal coordinates was employed in energy minimization and the default cutoffs were used throughout.[15] C_{4v} symmetry was detected for all the complexes in the input structures, and was then enforced by the program. By using the energy-minimized structures generated in the previous step, normal coordinate analyses were carried out. Charge distribution analysis was carried out using a full natural bond orbital (NBO) analysis population method based on the minimized structure. The primarily calculated vibrational frequencies were scaled by the factor 0.9614.[16] UV/Vis spectroscopic calculations were carried out by the TDDFT method. All calculations were carried out using the Gaussian 03 program[17] in the IBM P690 system in Shandong Province High Performance Computing Centre.

[(Pc)Y(TClPP)] was prepared according to the published procedure,[7i] and [(Pc)Y(TClPP)]$^-$ was obtained by reducing [(Pc)Y(TClPP)] with hydrazine hydrate. Electronic absorption spectra were recorded at room temperature on a Hitachi U-4100 spectrophotometer in chloroform.

Acknowledgements

[1] *The Porphyrin Handbook, Vols. 1–20* (Eds.: K. M. Kadish, K. M. Smith, R. Guilard), Academic Press, San Diego, **2000** and **2003**.

[2] T. Mashiko, D. Dolphin, in *Comprehensive Coordination Chemistry, Vol. 2* (Eds.: G. Wilkinson, R. D. Gillard, J. A. McCleverty), Pergamon, Oxford, **1987**, Chapter 21.1, p. 813.

[3] K. M. Smith, in *Comprehensive Heterocyclic Chemistry, Vol. 4* (Eds.: A. R. Katritzky, C. W. Rees), Pergamon, Oxford, **1984**, Chapter 3.07, p. 377..

[4] *The Porphyrins, Vols. 1–7* (Ed.: D. Dolphin), Academic Press, New York, **1978**.

[5] a) J. Jiang, K. Kasuga, D. P. Arnold, in *Supramolecular Photosensitive and Electroactive Materials* (Ed.: H. S. Nalwa), Academic Press, New York, **2001**, Chapter 2, pp. 113–210; b) D. K. P. Ng, J. Jiang, *Chem. Soc. Rev.* **1997**, *26*, 433–442; c) J. Jiang, W. Liu, D. P. Arnold, *J. Porphyrins Phthalocyanines* **2003**, *7*, 459–473; d) Y. Bian, J. Jiang, Y. Tao, M. T. M. Choi, R. Li, A. C. H. Ng, P. Zhu, N. Pan, X. Sun, D. P. Arnold, Z. Zhou, H.-W. Li, T. C. W. Mak, D. K. P. Ng, *J. Am. Chem. Soc.* **2003**, *125*, 12257–12267; e) J. Jiang, Y. Bian, F. Furuya, W. Liu, M. T. M. Choi, N. Kobayashi, H.-W. Li, Q. Yang, T. C. W. Mak, D. K. P. Ng, *Chem. Eur. J.* **2001**, *7*, 5059–5069; f) P. Zhu, N. Pan, R. Li, J. Dou, Y. Zhang, D. Y. Y. Cheng, D. Wang, D. K. P. Ng, J. Jiang, *Chem. Eur. J.* **2005**, *11*, 1425–1432; g) R. Wang, R. Li, Y. Bian, C.-F. Choi, D. K. P. Ng, J. Dou, D. Wang, P. Zhu, C. Ma, R. D. Hartnell, D. P. Arnold, J. Jiang, *Chem. Eur. J.* **2005**, *11*, 7351–7357; h) R. Wang, R. Li, Y. Li, X. Zhang, P. Zhu, P.-C. Lo, D. K. P. Ng, N. Pan, C. Ma, N. Kobayashi, J. Jiang, *Chem. Eur. J.* **2006**, *12*, 1475–1485.

[6] a) S. Yoshimoto, T. Sawaguchi, W. Su, J. Jiang, N. Kobayashi, *Angew. Chem.* **2007**, *119*, 1089–1092; *Angew. Chem. Int. Ed.* **2007**, *46*, 1071–1074; b) Y. Chen, W. Su, M. Bai, J. Jiang, X. Li, *J. Am. Chem. Soc.* **2005**, *127*, 15700–15701; c) T. Ye, T. Takami, R. Wang, J. Jiang, P. S. Weiss, *J. Am. Chem. Soc.* **2006**, *128*, 10984–10985; d) Y. Bian, X. Chen, D. Wang, C.-F. Choi, Y. Zhou, P. Zhu, D. K. P. Ng, J. Jiang, Y. Weng, X. Li, *Chem. Eur. J.* **2007**, *13*, 4169–4177; e) N. Ishikawa, T. Iino, Y. Kaizu, *J. Am. Chem. Soc.* **2002**, *124*, 11440–11447; f) N. Ishikawa, S. Otsuka, Y. Kaizu, *Angew. Chem.* **2005**, *117*, 741–743; *Angew. Chem. Int. Ed.* **2005**, *44*, 731–733.

[7] a) W. Liu, J. Jiang, D. Du, D. P. Arnold, *Aust. J. Chem.* **2000**, *53*, 131–136; b) J. W. Buchler, B. Scharbert, U. Englert, J. Strähle, *Chem. Ber.* **1988**, *121*, 2077–2082; c) G. A. Spyroulias, A. G. Coutsolelos, C. P. Raptopoulou, A. Terzis, *Inorg. Chem.* **1995**, *34*, 2476–2479; d) G. A. Spyroulias, C. P. Raptopoulou, D. de Montauzon, A. Mari, R. Poilblanc, A. Terzis, A. G. Coutsolelos, *Inorg. Chem.* **1999**, *38*, 1683–1696; e) J.-H. Agondanou, G. A. Spyroulias, J. Purans, G. Tsikalas, C. Souleau, A. G. Coutsolelos, S. Benazeth, *Inorg. Chem.* **2001**, *40*, 6088–6096; f) G. A. Spyroulias, A. G. Coutsolelos, *Inorg. Chem.* **1996**, *35*, 1382–1385; g) D. Chabach, M. Tahiri, A. De Cian, J. Fischer, R. Weiss, M. El Malouli Bibout, *J. Am. Chem. Soc.* **1995**, *117*, 8548–8556; h) J. Jiang, W. Liu, X. Sun, D. K. P. Ng, *Chem. Res. Chin. Univ.* **2001**, *17*, 134–142; i) F. Lu, X. Sun, R. Li, D. Liang, P. Zhu, X. Zhang, C.-F. Choi, D. K. P. Ng, T. Fukuda, N. Kobayashi, J. Jiang, *New J. Chem.* **2004**, *28*, 1116–1122.

[8] a) G. Ostendorp, H. Homborg, Z. *Anorg. Allg. Chem.* **1996**, *622*, 873–880; b) G. Ostendorp, H. Homborg, Z. *Anorg. Allg. Chem.* **1996**, *622*, 1358–1364; c) J. Jiang, W. Liu, J. Lin, D. K. P. Ng, *Huaxue Tongbao* **1997**, *7*, 14–19; d) Y. Zhang, X. Cai, Y. Zhou, X. Zhang, H. Xu, Z. Liu, X. Li, J. Jiang, *J. Phys. Chem. A* **2007**, *111*, 392–400.

[9] a) J. Jiang, R. C. W. Liu, T. C. W. Mak, T. D. W. Chan, D. K. P. Ng, *Polyhedron* **1997**, *16*, 515–520; b) J. Jiang, J. Xie, D. K. P. Ng, Y. Yan, *Mol. Cryst. Liq. Cryst. Sci. Technol. Sect. A* **1999**, 337–385; c) J. Jiang, J. Xie, M. T. M. Choi, S. Sun, D. K. P. Ng, *J. Porphyrins Phthalocyanines* **1999**, *3*, 322–328.

[10] J. Jiang, W. Liu, W. -F. Law, J. Lin, D. K. P. Ng, *Inorg. Chim. Acta* **1998**, *268*, 49–53.

[11] J. W. Buchler, J. Hüttermann, J. Löffler, *Bull. Chem. Soc. Jpn.* **1988**, *61*, 71–77.

[12] a) C. Lee, W. Yang, R. G. Parr, *Phys. Rev. B* **1988**, *37*, 785–789; b) A. D. Becke, *J. Chem. Phys.* **1993**, *98*, 5648–5652.

[13] a) P. J. Hay, W. R. Wadt, *J. Chem. Phys.* **1985**, *82*, 299–310; b) T. H. Dunning, Jr., P. J. Hay, in *Modern Theoretical Chemistry, Vol. 3* (Ed.: H. F. Schaefer III), Plenum, New York, **1976**.

[14] a) Y. Zhang, X. Zhang, Z. Liu, Y. Bian, J. Jiang, *J. Phys. Chem. A* **2005**, *109*, 6363–6370; b) Y. Zhang, X. Zhang, Z. Liu, H. Xu, J. Jiang, *Vib. Spectrosc.* **2006**, *40*, 289–298; c) X. Zhang, Y. Zhang, J. Jiang, *Vib. Spectrosc.* **2003**, *33*, 153–161; d) X. Zhang, Y. Zhang, J. Jiang, *Spectrochim. Acta Part A* **2004**, *60*, 2195–2200; e) X. Zhang, Y. Zhang, J. Jiang, *Spectrochim. Acta Part A* **2005**, *61*, 2576–2583.

[15] C. Peng, P. Y. Ayala, H. B. Schlegel, M. J. Frisch, *J. Comput. Chem.* **1996**, *17*, 49–56.

[16] NIST Computational Chemistry Comparison and Benchmark Database, NIST Standard Reference Database Number 101 Release 10, May **2004**, Editor: Russell D. Johnson III http://srdata.nist.gov/cccbdb.

[17] Gaussian 03 (Revision B.05), M. J. Frisch, G. W. Trucks, H. B. Schlegel, G. E. Scuseria, M. A. Robb, J. R. Cheeseman, J. A. Montgomery Jr., T. Vreven, K. N. Kudin, J. C. Burant, J. M. Millam, S. S. Iyengar, J. Tomasi, V. Barone, B. Mennucci, M. Cossi, G. Scalmani, N. Rega, G. A. Petersson, H. Nakatsuji, M. Hada, M. Ehara, K. Toyota, R. Fukuda, J. Hasegawa, M. Ishida, T. Nakajima, Y. Honda, O. Kitao, H. Nakai, M. Klene, X. Li, J. E. Knox, H. P. Hratchian, J. B. Cross, C. Adamo, J. Jaramillo, R. Gomperts, R. E. Stratmann, O. Yazyev, A. J. Austin, R. Cammi, C. Pomelli, J. W. Ochterski, P. Y. Ayala, K. Morokuma, G. A. Voth, P. Salvador, J. J. Dannenberg, V. G. Zakrzewski, S. Dapprich, A. D. Daniels, M. C. Strain, O. Farkas, D. K. Malick, A. D. Rabuck, K. Raghavachari, J. B. Foresman, J. V. Ortiz, Q. Cui, A. G. Baboul, S. Clifford, J. Cioslowski, B. B. Stefanov, G. Liu, A. Liashenko, P. Piskorz, I. Komaromi, R. L. Martin, D. J. Fox, T. Keith, M. A. Al-Laham, C. Y. Peng, A. Nanayakkara, M. Challacombe, P. M. W. Gill, B. Johnson, W. Chen, M. W. Wong, C. Gonzalez, J. A. Pople, Gaussian, Inc., Pittsburgh, PA, **2004**.